

Journal of Hydrosience and Hydraulic Engineering
Vol. 14, No. 2, November, 1996, 81-88

STUDY ON EFFECTS OF UPDRAFT ON PRECIPITATION PROCESSES USING TWO-DIMENSIONAL CUMULUS MODEL

By

Satoru Oishi

Disaster Prevention Research Institute, Kyoto University,
Gokasho, Uji, Kyoto 611, JAPAN

Yugo Kitani

Graduate School of Kyoto University, Yoshida Honmachi, Sakyo-ku,
Kyoto 606-01, JAPAN

Eiichi NAKAKITA and Shuichi IKEBUCHI

Disaster Prevention Research Institute, Kyoto University,
Gokasho, Uji,

SYNOPSIS

Effects of updraft, which is primarily caused by topography, on precipitation processes were investigated numerically. With the aid of a numerical simulation model, which utilizes detailed cloud microphysics and represents cold rain processes, positive correlation between updraft and rainfall was caught only when updraft speed is below a threshold. In other words, the results showed that there is a threshold of updraft speed that causes heavy rainfall and that any faster updraft would not cause heavier rainfall. This relationship is explained by referencing the results of simulation, which indicated that the existence of hail is important for heavy rainfalls.

INTRODUCTION

Numerical approach is an effective and important way to explain the phenomena in convective clouds which is difficult to observe when it occurs in a small area of mountainous topography. This study presents a numerical approach using a two-dimensional cumulus model in which the detailed cloud microphysics is represented explicitly, based on Takahashi and Awata (3). The cumulus model is suitable to study severe rainfall in Japan because it represents ice particles such as hail, graupel and ice crystal and it also explicitly represents the cumulus microphysical processes. Our two purposes of investigating with the cumulus model are: 1) to discuss the role of updraft as a trigger of cumulus, by investigating cloud microphysical processes and 2) to determine the characteristics of the time series variation and spatial distribution of rainfall for a mountainous area. Due to the characteristics of the model, the model makes it possible to express physically, the production of precipitation particles at each cumulus development stage, physically. The characteristics of the time series and spatial distribution are also discussed since the production ratio of each precipitation particle can be obtained. The discussion is based on the numerical results obtained through three cases; Case 1: with no initial updraft, Case 2: with weak initial updraft, and Case 3: with strong initial updraft. The discussion also focuses on the speed and scale of cumulus at the initial developing stage, the development speed of cumulus, and the rainfall intensity at ground level.

MODELING OF MICROPHYSICS

The cumulus model has both microphysical processes and dynamic processes (which are represented by the commonly used primitive equations). The computation area width of the model is 22km (400 m \times 55 grids) and its height is 9km (200m \times 45 grids). The computation flow of the simulation is accomplished by the following steps: [1] calculating wind vectors using dynamic equations, [2] calculating variations of water vapor mixing ratio and potential temperature through advection, [3] calculating variations of precipitation particles and nucleus through advection and diffusion, [4] calculating the pressure and adding its effect on the wind vectors, [5] calculating the variation of each variable in the microphysical processes, and [6] proceeding to the next time step by returning to [1]. The Anerastic (AE) equation system, using the Poisson equation for solving the pressure diagnostically, was used for the non-hydrostatic dynamic processes. The details of the dynamic processes, which is written on Takahashi (2), are not explained in this paper because they are relatively well-known.

Next, the microphysical processes for the precipitation particles used in the model is explained. The precipitation particles which are represented in this model are classified into four types as shown in Table 1. They are further classified into 45 classes (for water drops, hail and graupel) or 105 classes (for ice crystal) by the diameter and thickness of each type.

The microphysical interaction processes are shown in Fig. 1. The following processes, which are important for discussing the following contents, are explained; the nucleation, condensation and collection processes of the water drop ($2 \rightarrow 3$ in Fig. 1) and the freezing process of the water drop ($3 \rightarrow 4$ in Fig. 1). The remaining processes in Fig. 1 are explained in Takahashi (1), (2).

Table 1 The precipitation particles in the model

Particle Clasification	Particle State	Particle Shape	Particle density(g/cm ³)
water drop	liquid	sphere	1.0
hail	ice	sphere	0.9
graupel	ice	sphere	0.3
ice crystal	ice	circular	0.1

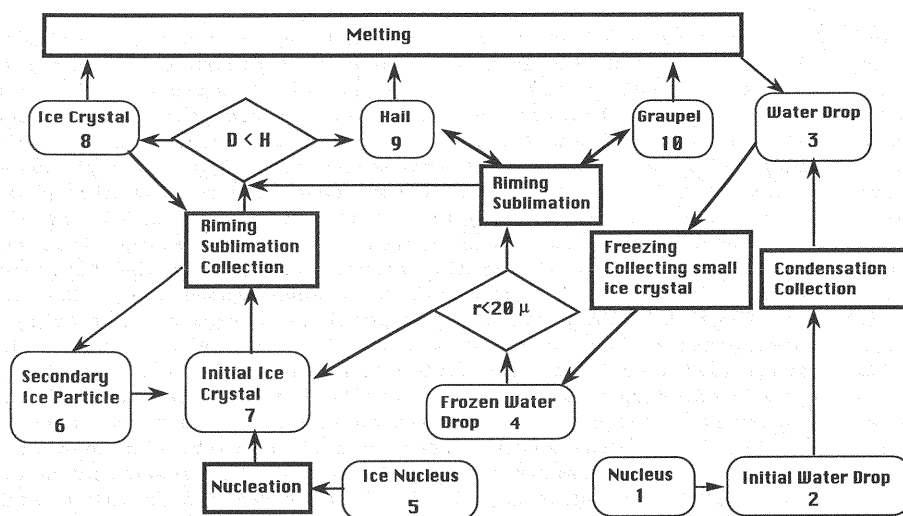


Fig. 1 Cloud microphysical interaction processes utilized in the model

Condensation, nucleation and collection processes of particles

Water vapor is changed to initial water drops through the process of nucleation. The initial water drops increase their size through condensation and collection. The rate of size increase of a water drop through condensation is represented by Eq. (1) which takes into account the following three factors: 1) water vapor diffusion ratio around the water drop, 2) increment of temperature by releasing latent heat and consequently, increasing saturated water vapor pressure and decreasing water vapor transport and 3) collection efficiency between molecules of water vapor and surface of water drop,

$$\frac{dm}{dt} = \frac{2\pi D(S-1)C_w}{\frac{L^2 M}{KRT_\infty^2} + \frac{RT_\infty^2}{e_s D_f M}} \quad (1)$$

where, m ; the mass of a water drop, S ; mixing ratio of supersaturated vapor, C_w ; ventilation coefficient, D ; diameter of a water drop, e_s ; saturation vapor pressure of the surrounding air, R ; gas constant, M ; molecule weight of water, T_∞ ; temperature of surrounding air, K ; thermal conductivity, L ; latent heat, and D_f ; diffusion coefficient of water vapor.

Using number density of water drops, $N(D)$ which is defined as the number of water drops having diameter D in a unit volume of air, Eq. (2) shows the mass increase of water in a unit volume of air,

$$\frac{dM}{dt} = \int_0^\infty \frac{2\pi D(S-1)C_w}{\frac{L^2 M}{KRT_\infty^2} + \frac{RT_\infty^2}{e_s D_f M}} N(D) dD \quad (2)$$

For processes other than the nucleation, the number density is calculated in this model. The condensation process mainly explains the growth of small water drops.

The Marshall-Palmer distribution is used as the water drop diameter distribution but only in the nucleation process since this distribution is difficult to calculate. Consequently, Eq. (2), the condensation equation for the nucleation process, becomes Eq. (3) for a unit volume of air,

$$\frac{dM}{dt} = \int_0^\infty \frac{2\pi D(S-1)C_w}{\frac{L^2 M}{KRT_\infty^2} + \frac{RT_\infty^2}{e_s D_f M}} N(D) dD = \frac{(S-1)C_w \cdot l_r^{0.525}}{5.5 \times 10^5 + (0.41 \times 10^7 / e_s)} \quad (3)$$

where, l_r is the mass of total water drops in a unit volume of air.

Growth of large water drops is primarily explained by the collection process. The number density, $n(x)$ which is a function of volume of a water drop, is used for calculation. The variation of number density of drop B , having volume b , by a collision between drops A , having volume a , and drop C , having volume $b-a$ is shown in Eq. (4),

$$\frac{\partial n(b)}{\partial t} = \frac{1}{2} \int_0^b n(a)V(b-a|a)n(b-a)da - \int_0^\infty n(b)V(b|a)n(a)da \quad (4)$$

where, $V(b|a)$ is a collection efficiency function which is a function of diameter of the water drop, the falling speed of the water drop and the projected area where drop A traps another drop.

Freezing process of a water drop

There are two processes in the freezing process of a water drop. One is freezing, and the other is contact nucleation. The empirical equation for freezing,

formulated by Vali (4) as the probability of freeze of a drop, is given by,

$$\xi_v = x_w \cdot \exp[-0.66(T-273)-1.0] \quad (5)$$

where, ξ_v represents the probability of supercooled drops freezing and x_w represents the mass of a water drop.

The contact nucleation process is one of the collection processes where a large water drop catches a relatively small ice particle and then the water drop becomes an ice particle. On the other hand, riming is defined as a collection processes where a large ice particle develops through catching a relatively small supercooled water drop. These collection processes are calculated using Eq. (4) in which the collection efficiency function is modified empirically. A frozen water drop is initially classified by its diameter and its density (to ice crystal if its diameter is less than 20 mm, to graupel if its diameter is larger than 20 mm and its density is greater than 0.3 g/cm³, and to hail if its diameter is larger than 20 mm and its density is greater than 0.9 g/cm³). Density of an ice particle is formulated as a function of falling speed and surface temperature. Ice crystals increase in their diameter through sublimation and increase in their thickness through riming. The other ice drops increase their diameter by sublimation, riming and aggregation.

EFFECTS OF UPDRAFT ON CUMULUS DEVELOPMENT

Modeling of initial updraft

Three types of initial updrafts (no updraft, weak one and strong one) were represented as initial dynamic conditions in the model. These initial updrafts can be explained as local updrafts which would blow due to the effect of mountainous topography. We investigated the effect of updraft on the cumulus developing processes, such as the nucleation process, enhancement of precipitation particles, and rainfall intensity at the ground level. It is noted that no dynamic process for keeping updraft is included in the model and wind is calculated using ordinal primitive equations.

Eq. (6) is a stream function in which the partial derivatives are taken, Eq. (7), and these derivatives represent the initial updraft. The reason for selecting the stream function is that the wind must satisfy the continuity equation Eq. (8).

$$\Phi = -A \sin\{\pi(x-2)/((X-2)/2)\} \sin\{\pi(z-1)/Z\} \quad (6)$$

$$u_0 = -\partial\Phi/\partial z, w_0 = \partial\Phi/\partial x \quad (7)$$

$$\partial(\rho u)/\partial x + \partial(\rho w)/\partial z = 0 \quad (8)$$

where, A represents a coefficient for wind speed, X represents the number of grids used in the computation area width (=55), and Z represents the number of grids used in the computation area height (=45).

Investigation of rainfall intensity under updraft condition

The investigation of the effect of updraft on rainfall intensity is based on the results of three cases. The maximum speed of the initial updraft for each case is 0 cm/s in Case 1, 20 cm/s in Case 2 and 40 cm/s in Case 3, which can be thought of as the no updraft case, the weak updraft case and the strong updraft case, respectively. All cases are calculated using same initial atmospheric circumstance except the wind profiles. A typical tropical summer profile, originally reported by Yamazaki (5) and modified by Takahashi and Awata (3), is used as a initial atmospheric profiles of this study to make calculation faster. Here, the effect of

existence and strength of updraft to rainfall intensity is discussed first. Then the cause of this result is investigated with respect to the concerned speed of cumulus development process and enhancement of precipitation particles in each microphysical process.

Time series variation of rainfall intensity at the ground level is shown in Fig. 2. This figure indicates the following characteristics of rainfall intensity. In Case 1, the rainfall area is narrow and the rainfall intensity is not strong. In Case 2, characteristics of initial rainfall are the same as in Case 1 (i.e. when $t = 20$ min.), however, the rainfall area is extremely wide and the rainfall intensity is stronger than in Case 1. In Case 3, the rainfall area is narrower than in Case 2 but a similar strong rainfall to Case 2 is shown. Cumulative rainfall of the three cases is shown in Fig. 3. This figure indicates that the cumulative rainfall decreases from Case 2, Case 3 and Case 1, in that specific order.

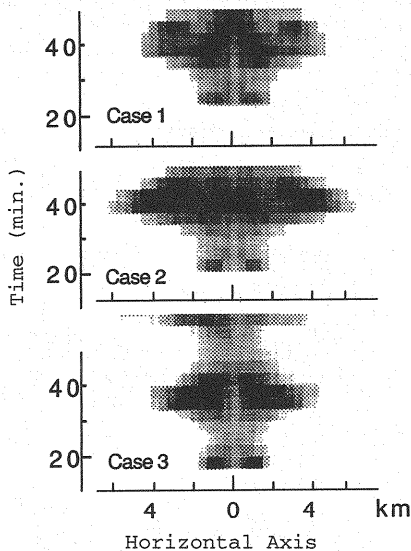


Fig. 2 Time series variation of rainfall intensity

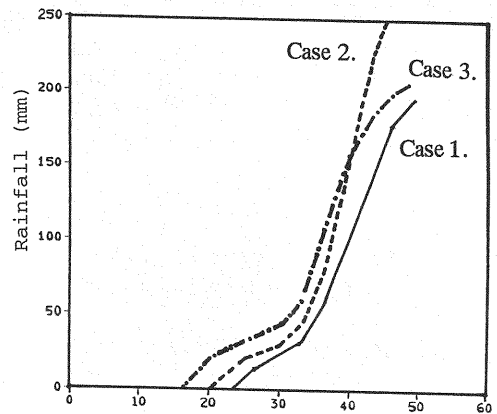


Fig. 3 Time series of cumulative rainfall

Generally speaking, it is agreed that the stronger the updraft, the heavier the resulting rainfall. It is consequently said that, if the horizontal wind is faster, the resulting rainfall will be heavier since faster horizontal wind creates stronger updraft due to the effect of mountainous topography. In other words, the relationship between rainfall intensity and initial updraft is thought to be positive correlation. However, as is found from the results of the three cases, the heavier rainfall does not result from the stronger updraft. Therefore, the relationship between rainfall intensity and initial updraft is not positive correlation. There is a certain speed of updraft that is recognized as the threshold, which is thought to be varied by atmospheric circumstance. When the initial updraft speed is below the threshold, the relationship between rainfall intensity and updraft is positive correlation, or in other words the heavier rainfall is caused from a stronger initial updraft. However, the positive correlation is not shown in the cases when the initial updraft is stronger than the threshold.

Investigation of relations between rainfall intensity and microphysical processes

Now the results of the three cases are investigated especially in terms of processes of cumulus development to further discuss the cause of the relationship

between rainfall intensity and microphysical processes. The understanding of the life stage of cumulus is important to discuss the detail of cumulus development. The cumulus life is classified to three stages; developing stage, mature stage and dissipating stage.

Initial updraft has a direct effect on the initial developing stage. Depending on the strength of the updraft, there is a variation that appears in the cumulus of the initial developing stage. The microphysical processes mainly propagate the initial variation of cumulus and then, they change the distribution of rainfall intensity. In case of no microphysical processes, initial updraft should be propagate slowly to the higher region (of the calculated area) since no dynamic processes for keeping updraft are included in the model. Contour (1.0×10^{-4} g/g) of mixing ratio of cloud drop (denoted by thin lines) and drizzle (denoted by thick lines) in the developing stage (at 800 sec) are shown in Fig. 4. Cloud drop is defined as a water drop having diameter of $2 - 32 \mu\text{m}$ and drizzle is defined as a water drop having diameter of $32 - 320 \mu\text{m}$. The height of cloud top and area of cloud in this figure indicates that development speed of initial cumulus decreases from Case 3, Case 2, Case 1, in that particular order. Although not shown here, the temperature resulting from release of latent heat in the cloud was also found to decrease from Case 3, Case 2, Case 1. It follows from the discussed fact that the relationships between development speed of cumulus in the initial developing stage and the speed of initial updraft is positive correlation.

Up until the mature stage, the following positive feedback process propagates the positive correlation between initial cumulus development speed and initial

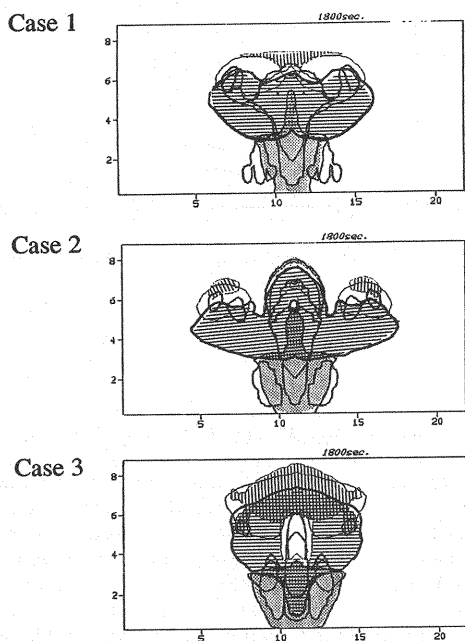


Fig. 4 Contour (1.0×10^{-4} g/g) of mixing ratio of cloud drop (denoted by thin lines) and drizzle (denoted by thick lines) in the developing stage (at 800 sec)

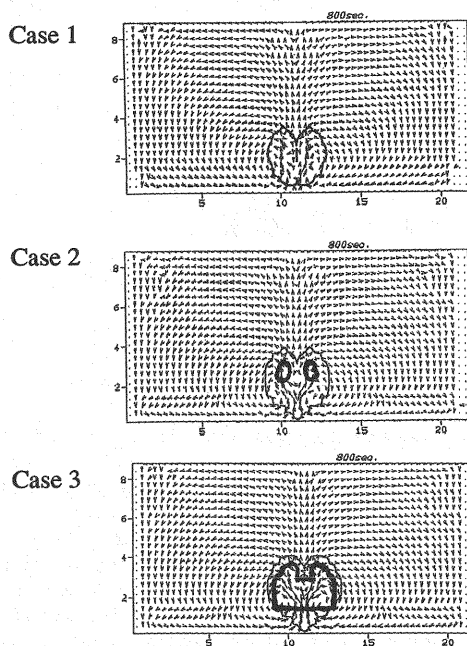


Fig. 5 Contour (1.0×10^{-4} g/g) of mixing ratio of rain drop (shaded by dots), hail (shaded by horizontal lines), ice crystal (shaded by vertical lines) and graupel (unshaded area between ice crystal and hail) in the mature stage (at 1800 sec)

updraft speed. The development of cumulus in the developing stage releases more latent heat by nucleation. This in turn causes the air in the cumulus to become lighter and more buoyant. The number of water particles created increases as the air is lifted higher. Some microphysical processes are activated by the increased precipitation particles which signify the beginning of the mature stage.

Contour (1.0×10^{-4} g/g) of mixing ratio of rain drop (shaded by dots), hail (shaded by horizontal lines), ice crystal (shaded by vertical lines) and graupel (unshaded area between ice crystal and hail) in the mature stage (at 1800 sec) are shown in Fig. 5. The rain drop is defined as a water drop whose diameter is larger than $320\mu\text{m}$. This figure indicates that hail is distributed widely in Case 2 and ice crystal is distributed widely in Case 3. Horizontal wind divergence, which is not shown in the figure, appears in the area where hail is distributed widely in Case 2. The divergence also appears at the area where ice crystals are distributed widely in Case 3. The wind divergence propagates each precipitation particle widely. The mechanism that causes the divergence is explained as follows. An air patch just above the cloud is lifted by an updraft due to the release of latent heat from the cloud. The temperature of the air patch decreases by dry adiabatic processes since it is not saturated. The air patch becomes consequently cooler than the surrounding atmosphere because the initial surrounding atmosphere is in a state of conditional unstable, inferring stable in the dry atmosphere. The cooled air patch is also the result of evaporation of the water drops at the top of the cloud. The cooled air patch will tend to have negative buoyancy since it is denser than the surrounding atmosphere. If the updraft is not strong enough to lift the air patch against the negative buoyancy of the cooled air patch, the cloud development process occurs horizontally and the wind divergence is created.

In Case 2, hail in the horizontally propagated cloud is pulled downwards by gravity and then becomes a rain drop since there is no updraft (from the release of latent heat) that supports the hail. In this mechanism, stored hails in the air become rain drops simultaneously and consequently heavy rainfall occurs. In Case 3, on the other hand, since the density of ice crystals is one seventh that of hail, the ice crystals in the propagated cloud will be pulled down at a slower rate since its terminal velocity, which is a function of density and diameter, is smaller than that of hail. Therefore, it is possible for an ice crystal to suspend in the air under the condition of no updraft and thus particles are kept suspended in the air longer time than in Case 2. It consequently rains weaker in Case 3 than in Case 2 because an ice crystal does not become a rain drop simultaneously like hail.

It deserves explicit emphasis that graupel and the riming play important roles for creating hail. Ice crystals are enlarged through the riming to form graupel. Graupel becomes hail through the riming, aggregation and sublimation. The updraft due to the release of latent heat from the cloud is so quick that water particles are brought to a higher region (of the calculated area) as in Case 3. There are no water drops in the higher region (of the calculated area) and the riming does not occur. In addition, the sublimation that occurs in the higher region enlarges the ice crystals slowly, therefore, a small amount of graupel is created by the sublimation and consequently the amount of hail is small in Case 3. Accordingly, the rainfall intensity is weaker and the cumulative rainfall is shorter in Case 3 than in Case 2.

CONCLUSIONS

In this study, we have discussed the relationship among initial updraft, rainfall intensity and cumulative rainfall by investigating the results of numerical simulations which included detailed cloud microphysics. From this discussion, it is concluded that: the relationship between initial updraft and rainfall intensity is not positive correlation. It can be also said that the relationship between initial updraft and cumulative rainfall is not positive correlation. At an threshold of initial updraft speed, rainfall intensity is heavier and cumulative rainfall is greater due to the widely propagated hails. Too strong initial updraft raise cloud higher and then only small amount of hail is created. It consequently does not increase the rainfall intensity and amount of cumulative rainfall. This conclusion lead us to recognize that observing hail is important to forecast severe rainfall occurring in small area (about $10\text{-}100\text{ km}^2$ considering the size of a cumulus)

and the observation is indispensable for the forecast having a lead time of no less than one hour.

REFERENCES

1. Takahashi, T. : Hail in an Axisymmetric Cloud Model, *Journal of Atmospheric Science*, No. 33, pp. 269-286, 1976
2. Takahashi, T. : *Cloud Physics*, Tokyodo Printing, 1987.
3. Takahashi, T. and Y. Awata : Cloud Development in a Two-Dimensional Cloud Model With Detailed Microphysics, *Annals, Disas. Prev. Res. Inst., Kyoto Univ.*, No.36 B 2, 1993
4. Vali, G. : Ice Nuclei Relative to Formation of Hail, *Science Report MW-58*, Stormy Weather Group, McGill University, Montreal, Canada, p. 51, 1968
5. Yamazaki, M. : A Further Study of the Tropical Cyclone without Parameterizing the Effects of Cumulus Convection, *Paper in Meteorology and Geophysics*, 34, pp. 768-776, 1983

APPENDIX - NOTATION

The following symbols are used in this paper:

A	= a coefficient for wind speed in Eq. (6);
C_w	= ventilation coefficient;
D	= diameter of a water drop;
D_f	= diffusion coefficient of water vapor;
e_s	= saturation water vapor pressure of the surrounding air;
K	= thermal conductivity;
L	= latent heat;
M	= molecule weight of water;
m	= mass of water vapor;
$N(D)$	= number of water drops having diameter D in a unit volume of air;
$n(x)$	= number of water drops having volume x in a unit volume of air;
R	= gas constant;
S	= mixing ratio of supersaturated vapor;
T	= temperature;
T_∞	= temperature of surrounding air;
$V(b/a)$	= collection efficiency function defined in Eq. (4);
x_w	= mass of water drop in Eq. (5);
X, Z	= number of grids used in the computation area width (=55), and height (=45), respectively;
x, z	= horizontal axis and vertical axis;
ρ	= density; and
ξ_v	= probability of supercooled drops freezing.

(Received January 18, 1996; revised September 28, 1996)